scientific reports

Check for updates

OPEN

First comparison of commercial systems to prepare nanofat: technical performances and biological quality differ among obtained products

Robin Arcani[1,2], Maxime Abellan[2,3], Stéphanie Simoncini[2], Vincent Dani[4], Stéphane Robert[2], Anouck Zavarro[2], Cécilia Bec[5], Elisabeth Jouve[6], Laurent Arnaud[7], Sophie Menkes[8], Guy Magalon[9], Romaric Lacroix[2,7], Françoise Dignat George[2,7], Florence Sabatier[2,5], Aurélie Daumas[1,2], Mélanie Velier[2,5,10] & Jérémy Magalon[2,5,10]✉

Nanofat is a relatively recent fat grafting technique obtained involving the mechanical emulsification of adipose tissue whose preparation is produced at the patient's bedside. Although it was initially reported to improve skin quality in intradermal applications, it is now increasingly used in regenerative medicine. However, the absence of standardized protocols and the diversity of commercial devices result in nanofat products of variable quality. This study presents the first comprehensive comparison of nanofat obtained from different commercially available preparation systems, combining both their technical performance and biological characterization. Lipoaspirates from five healthy donors were processed using eight commercially available devices for nanofat production using emulsification or micronization techniques. The technical parameters included preparation time, ease of preparation and injection, volumetric yield, and residual aqueous fraction. Biological analyses included stromal vascular fraction isolation with evaluation of cell viability, viable nucleated cell yield, immunophenotypic cell subtype characterization and clonogenic capacity. These parameters were compared using a scoring model that enabled inter-kit ranking, integrating both a technical performance score and a biological quality score. Additionally, nanofat-conditioned media were collected for extracellular vesicles (EVs) quantification and subtyping by flow cytometry, and confocal microscopy was performed to evaluate the preservation of mature adipocytes, capillary networks, and the extracellular matrix. All devices demonstrated satisfactory technical performance, with Puregraft Boost V2 and Emulsfat achieving the highest overall technical scores. Cell viability was consistently high, with median values above 85% across all devices. Adinizer provided the greatest proportion of adipose-derived stromal/stem cells and achieved the highest overall biological score. In contrast, Hy-Tissue Nanofat produced the lowest cell yields together with the highest leukocyte proportions. All nanofats contained clonogenic progenitors. Extracellular vesicles concentrations were comparable between devices, and were mainly influenced by donor variability, although Emulsfat was enriched in adipocyte-derived EVs. Microscopic analysis revealed preservation of adipocytes, vascular networks, and the extracellular matrix across devices, challenging the assumption that emulsification or micronization completely disrupts tissue architecture. Nanofat properties are strongly device dependent, with possible dissociation between

technical ease and biological quality. This first comparative study highlights the need for standardized preparation methods and qualification criteria, and provides guidance for selecting devices aligned with specific clinical objectives to optimize regenerative outcomes.

Keywords Nanofat, Stromal vascular fraction, Regenerative medicine, Adipose-derived stem cells, Fat grafting, Extracellular vesicles, Medical device

Abbreviations

AEVs	Adipocyte-derived extracellular vesicles
ASC	Adipose-derived stem/stromal cells
ASC-EVs	Adipose stromal/stem cell-derived extracellular vesicles
AT	Adipose tissue
ATMP	Advanced therapy medicinal product
CFU-F	Colony forming units-fibroblasts
CM	Conditioned media
DAPI	4',6-Diamidino-2-phenylindole (utilisé pour marquage nucléaire)
EBM	Endothelial basal medium
ECM	Extracellular matrix
EEVs	Endothelial-derived extracellular vesicles
ErEVs	Erythrocyte-derived extracellular vesicles
EVs	Extracellular vesicles
FBS	Fetal bovine serum
FMO	Fluorescence minus one
HSA	Human serum albumin
IFATS	International federation for adipose therapeutics and science
IGF	Insulin-like growth factor
IQR	Interquartile range
ISCT	International society for cellular therapy
LEVs	Leukocyte-derived extracellular vesicles
MSC-EVs	Mesenchymal stromal/stem cell-derived EVs
ORO	Oil Red O
PBS	Phosphate-buffered saline
PDGF	Platelet-derived growth factor
PEVs	Platelet-derived extracellular vesicles
PFA	Paraformaldehyde
SVF	Stromal vascular fraction
VEGF	Vascular endothelial growth factor
VNC	Viable nucleated cells

[1]Internal Medicine and Therapeutics Department, CHU La Timone, AP-HM, Marseille, France. [2]Aix-Marseille University, INSERM, INRAE, C2VN, Marseille, France. [3]Plastic Surgery Department, CHU Conception, AP-HM, Marseille, France. [4]ExAdEx-Innov, 28 Avenue de Valombrose, Nice, France. [5]Laboratoire de Culture et Thérapie Cellulaire, Cell Therapy Department, CHU de La Conception, INSERM CIC BT 1409, 147 Boulevard Baille, AP-HM, 13005 Marseille, France. [6]Clinical Pharmacology and Drug Surveillance, Marseille University Hospital, Marseille, France. [7]Department of Hematology, Biogenopole, CHU La Timone, APHM, Marseille, France. [8]Centre for Aesthetic & Regenerative Medicine, Clinique Genolier, Genolier, Switzerland. [9]Remedex, Regenerative Medicine Department of Excellence, Marseille, France. [10]These authors contributed equally: Mélanie Velier and Jérémy Magalon. ✉email: jeremy.magalon@ap-hm.fr

Autologous adipose tissue (AT) has long been recognized as an ideal soft tissue filler because of its ease of harvest, abundance, and excellent biocompatibility, leading to its widespread use in plastic and reconstructive surgery[1–3]. Building on these advantages, Sydney Coleman pioneered a major breakthrough in 1995 by developing and standardizing a technique for injecting autologous human adipose tissue using a blunt tip harvesting cannula (3 mm diameter, with two facing orifices larger than 2 mm)[4]. Initially applied as millifat to restore volume in cases of tissue damage from trauma, disease, or aging, AT grafting has progressively revealed additional trophic effects on the skin[1,5]. These regenerative properties have been attributed to the presence of regenerative cells within the AT, including adipose-derived stromal/stem cells (ASC)[6].

To extend adipose grafting to thiner anatomical structures and achieve regenerative rather than purely volumizing effects, alternative forms based on the use of harvesting cannula with a diameter of 2 mm and orifices measuring around a millimeter referring to microfat[7] have been developed. More recently, nanofat, generated through a purely mechanical process without enzymatic digestion, has been described by Tonnard et al.[8] and is used for the treatment of the superficial layers of the skin[5].

According to current European Union Regulation 1394/2007 (and associated guidelines on human cells and tissues), nanofat is not considered as an Advanced Therapy Medicinal Product (ATMP), since its preparation does not involve substantial manipulation and its subcutaneous use is homologous. Consequently, nanofat falls within the scope of a routine clinical procedure rather than ATMP regulation. The classical technique for nanofat production involves repeated emulsification by passing the harvested fat between syringes through a connector, followed by filtration through a mesh of defined pore size. This method produces a supposed adipocyte-free,

liquid-like emulsion enriched in regenerative cells, including ASC and endothelial progenitor cells[10]. Tonnard et al. reported that the injection of nanofat into the superficial layers of the skin, improved skin rejuvenation by stimulating collagen synthesis and tissue remodeling[8]. Importantly, nanofat also retains microfragments of connective tissue with preserved vascular niches and native extracellular matrix, which could contribute to its regenerative potential[11].

Nanofat's biological activity is attributed to both its cellular and paracrine content, as it contains ASC, endothelial progenitor cells, endothelial cells, macrophages, lymphocytes, pericytes and preadipocytes[12–14]. Moreover, nanofat- conditioned medium (referred also to as "secretome") is rich in bioactive factors with proliferative, pro-angiogenic, pro-differentiating, anti-inflammatory, and anti-apoptotic properties. These include growth factors such as platelet-derived growth factor (PDGF), vascular endothelial growth factor (VEGF) and insulin-like growth factor (IGF) as well as bioactive peptides and cytokines[10,11,13,15]. Although some evidence suggests that mechanical shear stress during emulsification may increase regenerative potential[13,14], comprehensive data on the biological content and performance of nanofat remain limited.

Owing to its simple and rapid preparation compatible with intraoperative workflows, nanofat has gained increasing interest for aesthetic, reconstructive, and regenerative applications[12,15–18]; particularly in situations where millifat or microfat are unsuitable, such as superficial facial layers or fibrotic tissues. This growing interest has driven the development of numerous medical devices specifically designed for nanofat production, highlighting its expanding role across various medical fields. Beyond simple emulsification kits, this momentum has also led to the emergence of new mechanical preparation systems, based on a micronization process in which AT is forced through sharp grids with orifices ranging from 2400 to 100 microns. Currently, more than ten commercial kits are available on the market, each which relies on distinct emulsification or micronization protocols. These procedures vary widely in terms of the number of passes, the diameter and type of connectors/sharps used between syringes, and the filtration systems employed or not (e.g., the presence and nature of the filter membrane). This procedural variability raises concerns regarding the comparability of nanofat preparations across studies, as the resulting products may differ substantially in their cellular and molecular composition, potentially altering their regenerative capacity[10,14] and the reproducibility of the results across studies.

Despite its clinical popularity, nanofat remains poorly defined and insufficiently standardized in the scientific literature. Variability in preparation protocols—from the number of emulsifications passes to the type of filtration device—along with the lack of consensus terminology hinder the reproducibility and interpretation of results. There are only few studies assessing the impact of nanofat processing on its regenerative properties[19–21]. Furthermore, most of the in vitro studies published to date have used non-commercial devices, further complicating comparisons and limiting the extrapolation of data[18].

To date, no standardized framework exists to compare nanofat preparation devices across both technical and biological domains. Our study aims to address this gap by comparing the technical performance and biological features of nanofat obtained with several widely used commercial systems. To provide an integrated and clinically meaningful overview of device performance, we developed a multidimensional scoring system intended to guide physicians who routinely use nanofat. Finally, we also aimed to investigate the histological microstructure of nanofat and to analyze the extracellular vesicles (EVs) content of its secretome.

Methods

Study design

Figure 1 illustrates the study design, which is based on a comparison of eight different nanofat medical devices across multiple technical and biological parameters (including both cellular and EVs characterization) and microscopic analysis.

Adipose tissue collection

The AT of healthy donors was obtained from surgical waste in the Department of Plastic Surgery, La Conception University Hospital, Marseille, France. Patients underwent surgery for aesthetic purposes. Donors did not suffer from any tumoral, vascular, inflammatory or metabolic disease. All adult donors who participated in the study received a written information, signed a consent (non-opposition notice) and did not express any objection to the use of their AT in accordance with French national regulation for the use of surgical waste. This study was approved by the Institutional Review Board of Assistance Publique—Hôpitaux de Marseille (GDPR number PADS25-25) and the local Ethics Committee (CSE25-88). The study was conducted according to the Declaration of Helsinki. The AT was harvested from subcutaneous locations and subfascial locations via liposuction from multiple locations, including the lumbar region, peritrochanteric area, gluteal region, inner thigh, medial knee, and abdomen. The harvested tissue was then pooled into a single, closed transportation pocket for each patient. AT harvesting was performed in an operating room under general anesthesia after standardized aseptic skin preparation using a 3 mm 11 Gauge Coleman cannula for millifat (2×4 mm $\times$ 2 mm holes) and a 2mm 14 Gauge St'rim cannula (8×0.94 mm $\times 0.77$ mm holes, Thiebaud, Margencel, France) for microfat. Millifat and microfat were collected through a closed circuit, preventing contamination of the harvested product. Once harvesting was complete, AT was transported to the cell therapy unit and the AT was immediately processed.

Nanofat preparation

Millifat and microfat samples were washed twice with Ringer Lactate solution to remove red blood cells, cellular debris, and residual infiltration fluid. Eight commercially available nanofat preparation systems were included in the comparison: Hy-Tissue Nanofat (Fidia, Abano Terme, Italy), Tulip Nanofat Kit (Tulip Medical, San Diego, CA, USA), Emulsfat (Benew Medical, Melesse, France), Microlyzer (T-Lab, Nilüfer, Turkey), Puregraft Boost V1 and Puregraft Boost V2 (Bimini HealthTech, Plano, TX, USA), LipoCube Nano (Lipocube, London, UK), and Adinizer (BSL, Busan, Republic of Korea). Notably, during the course of the study, Bimini Healthtech released

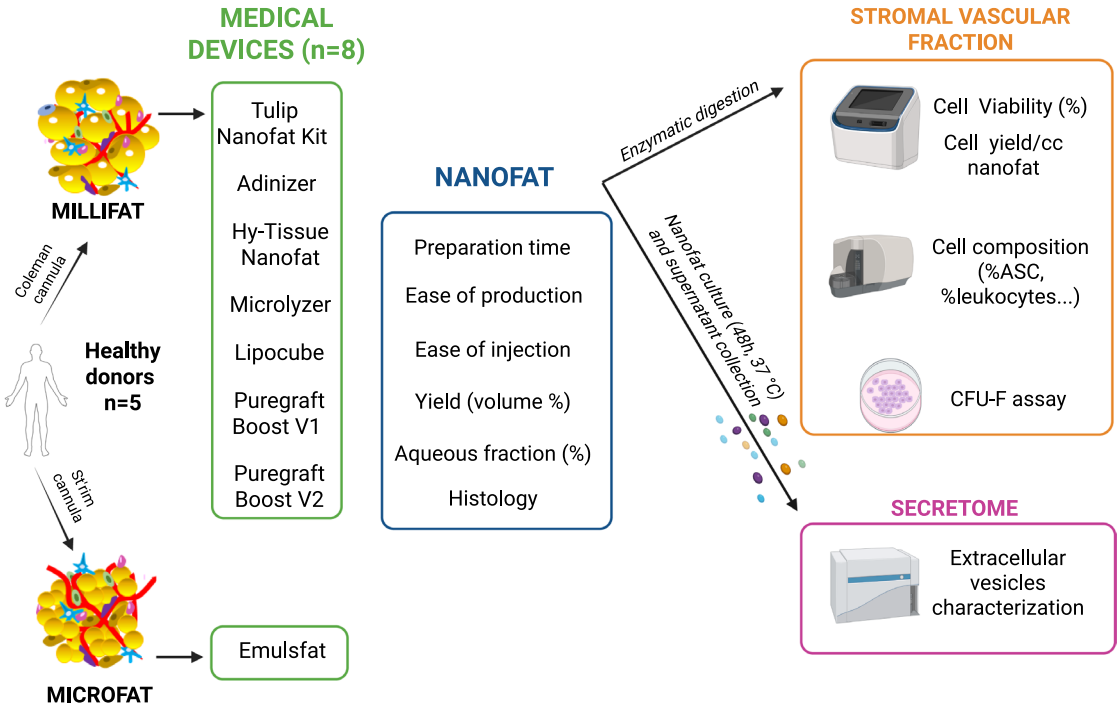

Fig. 1. Study design. Nanofat was prepared from lipoaspirates collected from five healthy donors via eight commercially available medical devices. All the devices processed millifat, except the Emulsfat system, which was applied to microfat. Multiple technical parameters were assessed for each preparation, including processing time, feasibility of production and injection, volumetric yield, proportion of the aqueous fraction, and histological features. In parallel, the stromal vascular fraction (SVF) was isolated from nanofat through enzymatic digestion and analyzed for cell viability, cell yield, immunophenotypic composition (flow cytometry), and clonogenic potential (CFU-F assay). Finally, the nanofat-derived secretome was characterized with a specific focus on extracellular vesicles, including their quantification and subpopulation distribution. Figure created with BioRender.com.

a revised version of its system (so called Puregraft Boost V2 in this study), incorporating design adaptations for professional use and an optimized working volume. Nanofat was primarily prepared from millifat, with the exception of the Emulsfat system, which utilizes microfat as its starting material. For each device, the emulsification/micronization protocol was followed during the preparation process. A summary of the main technical characteristics of each system is provided in Table 1.

Assessment of technical parameters related to nanofat preparation and administration

Time of preparation

The preparation time was measured from the opening of the preparation device to the end of production, following the supplier's instructions for each experiment by an independent operator.

Assessment of preparation ease

The ease of preparation of each nanofat using each of the evaluated kits was assessed by specialists in regenerative medicine. All steps of nanofat preparation were performed by the same trained operator to ensure consistency and eliminate inter-manipulator variability. At the end of each preparation, the operator rated the overall ease of use of the system on a 6-point Likert scale ranging from 0 (major issue encountered such as device obstruction or inability to complete the process) to 5 (very easy to use). A score of 5 was assigned when the system was intuitive to use, required minimal force during manipulation, and allowed a smooth workflow without interruption. This standardized assessment enabled objective comparisons of user-friendliness across the different preparation systems.

Assessment of injection ease

The ease of injection of nanofat prepared with each of the studied kits was assessed via the *Professional Skin Pad Mk 3* (Adam, Rouilly, UK), a synthetic model designed to mimic the consistency of human skin and ensure standardized injection conditions. A fixed volume (0.5 ml) of nanofat was injected using a 1 mL syringe equipped with a 30-gauge cannula. Injections were performed independently by three blinded experienced healthcare professionals under identical conditions. Following each injection, the evaluators rated injection ease using a 6-point Likert scale ranging from 0 (very difficult) to 5 (very easy). The rating was based on injection smoothness, perceived resistance during plunger depression, and the absence of blockage. An injection was considered "very easy" when it was performed smoothly, without obstruction or the need for significant pressure

	Tulip nanofat kit (tulip medical)	Adinizer (BSL)	Hy-tissue nanofat (Fidia)	Microlyzer (T-lab)	LipoCube nano (Lipocube)	Puregraft Boost V1 (Bimini HealthTech)	Puregraft Boost V2 (Bimini HealthTech)	Emulsfat (Benew Medical)
Starting material for preparation	Millifat	Millifat	Millifat	Millifat	Millifat	Millifat	Millifat	Microfat
Syringes for preparation	10 cc	20 cc	10 cc	10 cc	10 cc	20 cc	10 cc	10 cc
Type of production	Emulsification	Micronization	Emulsification	Micronization	Emulsification/Micronization	Micronization	Micronization	Emulsification
Number of connectors	2	4	1	3	3	2	2	1
Diameter (and type) of connectors	2.4 mm (hole) 1.2 mm (hole)	2.4 mm (blades) 1.2 mm (blades) 0.6 mm (blades) 0.4 mm (blades)	1.9 mm (hole)	2.4 mm (blades) 1.2 mm (blades) 0.6 mm (blades)	1.0 mm* (blades) 4.5 mm (hole)** 0.5 mm (blades)***	1.5 mm (blades) 0.5 mm (blades)	1.5 mm (blades) 0.5 mm (blades)	1.6 mm (hole)
Number of passes per connector	30	5	30	10	1* 10** 1***	10	10	10
Filtration	Yes	No	Yes	No	No	No	No	Yes
Size (and type) of filters	0.6 and 0.394 mm (double layered screen)	NA	0.12 mm (inner bag)	NA	NA	NA	NA	0.4 mm (screen)
Surface of filter (cm^2)	3	NA	2 × 25	NA	NA	NA	NA	9

Table 1. Comparative technical specifications of nanofat preparation devices. *NA* not applicable.

on the plunger. This protocol enabled an objective comparison of injection ease between the different nanofat preparation kits, while accounting for inter-evaluator variability.

Volumetric yield assessment

The volumetric yield of nanofat was calculated for each preparation system by dividing the final volume of nanofat obtained by the initial volume of adipose tissue processed—either millifat or microfat, depending on the specific requirements of each kit. This ratio, expressed as a percentage, reflects the efficiency of each system in converting washed AT into usable nanofat.

Assessment of the residual aqueous fraction

To evaluate the proportion of residual aqueous phase in the different nanofat preparations, a volume of 1 mL from each sample was centrifuged at 470 × g for 10 min at room temperature, without braking in order to produce phase separation. Representative images of the resulting layers were captured and analyzed using Fiji (ImageJ) by three independent operators (see Supplementary Figure S1 as a representative image of phase separation used for quantification). The proportion of aqueous fraction was quantified by calculating the ratio between the area of the aqueous layer and the total cross-sectional area, expressed as a percentage.

Assessment of the biological parameters of nanofat-derived cells

Enzymatic digestion

To determine the biological features of the cells contained within the different products; a standardised volume of 3 mL of nanofat obtained through the eight procedures were enzymatically digested with 0.25 U/mL collagenase NB4 (Nordmark Pharma GmbH, Uetersen, Germany) for 45 min at 37°C. Enzymatic digestion was stopped with sterile, clinical grade 5% human serum albumin (HSA, VIALEBEX), and the cells were subsequently centrifuged at 500×*g* for 5 min. The resulting cells in the pellet, i.e., the Stromal Vascular Fraction (SVF), were resuspended in 5% HSA and filtered with 70 µm filter.

Cell numeration and viability

The number of viable nucleated cells (VNC) and the percentage of viable cells were determined using a Luna Fx7 automatic cell counter (Logos Biosystems, Anyang, Republic of Korea). The yield was calculated as the total number of VNC obtained divided by the total volume of nanofat obtained after manufacturing. Cell viability and yield were included for the biological scoring.

Flow cytometry analysis of cell subsets

Characterization of the SVF cell subpopulations was performed by flow cytometry, also using a 10-channel Navios device (Beckman Coulter, Brea, CA, USA). For each nanofat, 500,000 cells were resuspended in phosphate-buffered saline (Gibco, Thermo Fisher Scientific, Waltham, MA, USA) and stained for 20 min at room temperature in the dark with a panel of cell surface markers according to the recommendations of the International Federation for Adipose Therapeutics and Science (IFATS) and the International Society for Cellular Therapy (ISCT)[22]. A mix of monoclonal antibodies conjugated to the corresponding fluorochrome was used: CD45-PC5, CD34-ECD, CD90-FITC, and CD146-PE (Beckman Coulter) in combination with the nuclear marker DRAQ5 (Thermo Fischer Scientific, Waltham, MA, USA). The red blood cells were lysed in NH4Cl for

10 min before the cells were centrifuged and resuspended in Phosphate-Buffered Saline (PBS). Then, NucBlue (Thermo Fisher Scientific), which allows differentiation between viable and dead cells, was added for 5 min prior to flow cytometry analysis. Data were analysed using Kaluza software (Beckman Coulter) according to the gating strategy (see supplementary Figure S2). The different cell subtypes were identified according to the following immunophenotypic profiles: leukocytes: $CD45^+/CD34^-$, endothelial cells: $CD45^-/CD34^+/CD146^+/CD90^-$ and adipose stromal/stem cells (ASC): $CD45^-/CD34^+/CD146^-/CD90^+$. Proportions of ASC and leukocytes within the SVF-derived nanofat were included for biological scoring.

Clonogenic assay CFUF

The clonogenic potential of SVF obtained from the different devices was evaluated by CFU-F (Colony Forming Units – Fibroblasts) assay. CFU-F colonies mainly derived from mesenchymal stromal/stem cells progenitors (fibroblast-like colonies). SVF cells were seeded in a six-well plate in triplicate (500 viables cells/plate) in the following medium: DMEM : 45% /HAMS-F12 : 45% (Gibco) supplemented with 10% fetal bovine serum (Biosera, Nuaillé, France), GlutaMAX® (100X, Gibco) and antibiotics. The medium was enriched with human serum albumin (HSA, VIALEBEX, final concentration 1%) for the first 5 days of culture, after which the medium (without HSA) was changed every 2–3 days. The colonies were then grown for 14 days. At the end of the experiment, the culture dishes were rinsed twice with phosphate buffered saline (Gibco), fixed with 10% neutral buffered formalin for 20 min and then stained with 0.5% crystal violet (Sigma-Aldrich, Merck KGaA, Darmstadt, Germany). Cell colonies were counted using phase contrast microscopy (EVOS™ M5000 Imaging System, Thermo Fisher Scientific). All three culture dishes were counted and the average and standard deviation were calculated to obtain the final percentage abundance value, which is expressed as the colony-forming efficiency divided by the number of seeded cells × 100).

Secretome and EVs quantification

Preparation of nanofat-conditioned medium

One milliliter of nanofat (produced by each device) was cultured with 9 mL of medium with Endothelial Cell Basal Medium (Pelobiotech GmbH, Planegg, Germany) supplemented with 0.5% fetal bovine serum (FBS). Cultures were incubated for 48 h at 37°C in a humidified atmosphere containing 5% CO_2. After incubation, the nanofat-conditioned medium (CM) was subjected to a serial centrifugation protocol to eliminate contaminating cells, debris, and apoptotic bodies. First, the samples were centrifuged at 300 × g for 10 min, and the resulting supernatants were then centrifuged at 2500 × g for 10 min. Following centrifugation, the supernatants were filtered through a 70 µm cell strainer (Corning Inc., Corning, NY, USA) to remove residual tissue fragments. Processed CM samples were stored at −20 °C until further analysis, limiting the number of freeze-thaw cycles to a maximum of one.

Flow cytometry for extracellular vesicles (EVs) identification and subtyping

EVs analysis by flow cytometry was performed using a 4-laser CytoFLEX S cytometer (Beckman Coulter) provided with a plate reader. To ensure consistent sizing and accurate gating of EVs, Megamix-Plus FSC/SSC fluorescent bead mixtures (BioCytex, Marseille, France) were employed. This standardized mixture of FITC-labeled polystyrene beads has defined diameters of 0.1, 0.16, 0.22, 0.24, 0.3, 0.5, and 0.9 µm, enabling precise calibration of the flow cytometer's scatter parameters. Although the FBS used in the endothelial basal medium (EBM)- 0.5% FBS medium was not EV-depleted, all these antibodies were specific to human species. We found that detection of EVs was negligible in the vehicle medium of nanofat-conditioned medium (EBM-0.5%FBS) *(data not shown)*. Based on established protocols[23], a gating strategy focusing on large EVs was implemented by defining a VSSC-FSC window corresponding to bead-equivalent diameters between 0.16 µm and 0.5 µm and minimizing background noise from smaller particles and debris. The concentration of EVs was determined by measuring the sample volume via CytoFLEX. Prior to staining, all the antibodies were centrifuged at 13,000×*g* for 2 min to remove the aggregates.

For each sample, 30 µL of CM was incubated with 10 µL of FITC-conjugated Annexin V (Tau Technologies) and 2.5 µL of each antibody targeting surface markers, including: CD41-APC (BioLegend), CD90-PC7 (BioLegend), CD49e-BB700 (BD Biosciences), CD73-brilliant violet 421 (BioLegend), CD235a-APC7 (BioLegend), CD146-PE (Biocytex) and CD45-PC5 (BioLegend). Antibody titrations were performed using nanofat-derived Annexin V^+ EVs to determine the optimal staining concentrations. The selected concentrations corresponded to those producing the highest percentage of Annexin V^+/antibody$^+$ EVs among total Annexin V^+ EVs. Following a 20-min incubation at room temperature, samples were diluted in 150 µL of Annexin V binding buffer and immediately analyzed. To prevent carryover, a dedicated wash well was used between each sample.

Gating strategy and subpopulation identification

EVs were initially gated based on Annexin V positivity, indicating exposure of phosphatidylserine. Fluorescence Minus One (FMO) controls were included for each marker to determine accurate positivity thresholds. EVs subtypes were identified according to the following immunophenotypic profiles: Platelet-derived EVs (PEVs): Annexin V^+ / $CD41^+$, Erythrocyte-derived EVs (ErEVs): Annexin V^+ / $CD235a^+$, Leukocyte-derived EVs (LEVs): Annexin V^+ / $CD45^+$, Endothelial-derived EVs (EEVs): Annexin V^+ / $CD146^+$ / $CD90^-$, Adipocyte-derived EV (AEVs): Annexin V^+ / $CD49e^+$ and Adipose mesenchymal stromal/stem cell-derived EVs (MSC-EVs): Annexin V^+ / $CD90^+$ / $CD73^+$. EVs concentrations are expressed as number of EVs per microliter (EV/µL), and subpopulation frequencies are reported as a percentage of Annexin V^+ EVs.

Microscopic analysis

Two groups of samples were compared against their own reference groups (lipoaspirates without manipulation). Millifat samples were compared with Tulip Nanofat Kit, Adinizer, Microlyzer, LipoCube Nano, Puregraft Boost V1 and Puregraft Boost V2, whereas microfat samples were compared with Emulsfat.

Immunofluorescence

Samples were fixed with 4% PFA in 1X PBS for 24 h at + 4°C under agitation, and then stored for future immunostaining analysis. Samples were processed for immunofluorescence as following. Samples were permeabilized (100X Triton 1% in 1X PBS) for 2 h at room temperature under agitation. For adipocytes, lipid droplets were stained with Oil Red O (ORO), and nuclei were stained with DAPI. For endothelial and laminin networks samples were incubated overnight at 4°C with primary anti-CD31 (Abcam ab28364) and anti-laminin (Abcam ab11575), and then for 45 min at room temperature with the corresponding secondary antibody. For clarification, samples were then dehydrated using increasing concentration of methanol (25%, 50%, 75% and 100%) for 15 min each at room temperature under agitation. Finally, the samples were cleared using Benzoic Acid Benzyl Benzoate (BABB) solution until transparency. Samples were visualized on an LSM 710 NLO inverted Axio Observer Z1 confocal microscope (Carl Zeiss Microscopy GmbH, Jena, Germany) using a Plan Apo 25 × or 10X multi-immersion (oil, glycerol, water) NA 0.8 objective and confocal images of the stained samples were acquired.

Adipocyte size measurement

A minimum of 3 fields of 250 μm^2 of confocal images or 1 larger field of 1000 μm^2 were used for analysis. At least 180 adipocytes were visualized and used for the analysis. Raw data of areas of ORO-stained objects were obtained by using Zen software (Zeiss), which corresponds to adipocytes ORO-stained objects separated into two subpopulations for segmentation of large (objects with an area > 30 000 $pixel^2$) and small (objects with an area < 30 000 $pixel^2$) objects. Minimal threshold for ORO-stained object was set up at 500 $pixel^2$. The raw data were processed to eliminate overlaps between objects. The area values were converted into μm^2 and diameter was calculated. The distribution of objects according to diameter was reported.

Quantification of endothelial (CD31) and extracellular matrix (Laminin) networks

Using Imaris software (Oxford Instruments, Zürich, Switzerland), corresponding surfaces regarding CD31 or laminin stainings were created. Surface volumes were calculated and normalized to the total volume of each image corresponding to the "normalized positive volume". For laminin staining, the laminin volume was normalized to the CD31 volume and the total volume of the image.

Statistical analysis

Statistical differences were evaluated by Kruskal–Wallis tests to assess differences between the eight devices for each quantitative variable (degree of freedom = 7). When significant, post-hoc pairwise comparisons were performed using Dunn's test (only significant *p*-values are presented). Technical and biological scoring of the eight commercially available nanofat processing devices were based on five parameters for each scoring. To facilitate comparative analysis across parameters with heterogeneous units and scales, a quantile-based scoring system was employed. Each parameter was independently categorized according to the quartiles, with discrete values assigned as follows: 0.25 (lowest quartile), 0.5 (second quartile), 0.75 (third quartile), and 1.0 (highest quartile), where higher values consistently represent superior performance. For parameters where lower values indicate better performance—specifically time of preparation, proportion of aqueous phase and proportion of leukocytes—the ranking was performed in reverse order (i.e., lower values assigned higher ranks) to maintain consistency in the scoring directionality. Two sub-scores (technical and biological scores, ranging from 1 to 5) were obtained for each preparation system. This quantile-based scoring approach yielded a normalized, interpretable dataset, facilitating multicriteria radar plot visualizations and enabling robust comparative assessments. Statistical analysis was performed using GraphPad Prism 10 (GraphPad Software). The data are presented as median [interquartile range (IQR)]. *P* values < 0.05 were considered statistically significant.

Results

Donor characteristics

Five healthy donors were included in the study from April 2023—March 2024 (five women, age range: 21–65 years; mean age ± SD: 39 ± 17 years, body mass index range : 28–37; mean body mass index ± SD : 29.6 ± 3.5kg/m^2. Adipose tissue was harvested from various anatomical regions including the abdomen (n = 4), flanks (n = 4), inguinal areas (n = 1), trochanters (n = 3), and inner sides of the thighs and knees (n = 1), by the same surgeon in all cases.

Technical performance assessment and ranking of commercial devices for nanofat production

The scores and radar plots for each device are presented in Fig. 2A,B. These results indicate that all devices showed good technical performance (with scores for all devices > 2.5/5). Ultimately, the highest technical scores are attributed to Puregraft Boost V2 and Emulsfat with a total score of 4.25 and 4.5/5 respectively. The fastest preparation times were observed with Puregraft Boost V2 (1.22 [0.93] minutes), while Hy-Tissue Nanofat required more than 4 min. Devices such as Adinizer, Hy-Tissue Nanofat, Puregraft Boost V2 and Emulsfat obtained high scores (over 4/5) for both ease of preparation and ease of injection, reflecting superior handling characteristics. In terms of volumetric yield, Tulip Nanofat Kit, Emulsfat and Microlyzer outperformed other systems with yields greater than 80%, suggesting a higher efficiency in nanofat volume. Moreover, Emulsfat presented the

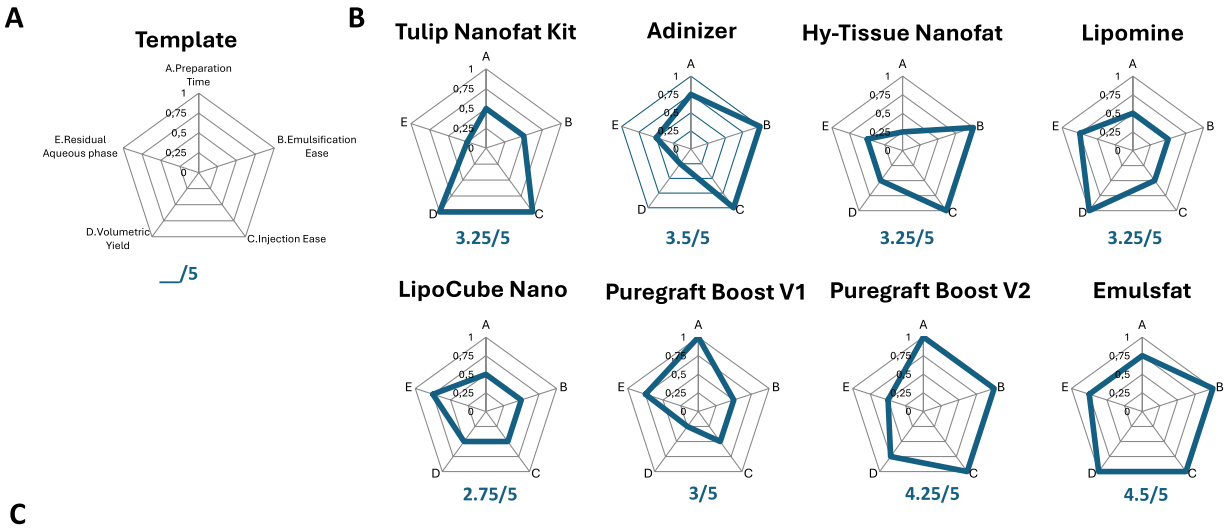

C

Parameter	Tulip Nanofat (n=5)	Adinizer (n=5)	Hy-Tissue Nanofat (n=5)	Lipomine (n=5)	LipoCube Nano (n=5)	Puregraft Boost V1 (n=4)	Puregraft Boost V2 (n=4)	Emulsfat (n=5)	*p*-value (Kruskal-Wallis)	Significant post-hoc *p*-value
Technical parameters										
Preparation time (min). Median [IQR]	3.31 [3.13]	2.58 [2.16]	4.53 [1.32]	3.25 [3.31]	3.01 [5.48]	1.79 |1.12]	1.22 |0.93]	2.59 [2.9]	**0.012**	Hy-Tissue Nanofat > Puregraft Boost V2 (p = 0.026)
Ease of preparation (Likert scale). Median [IQR]	3 [3.25]	4 [1]	4 [1]	2 [4]	3 [4]	2.75 [1.25]	4 [1.13]	4 [5]	0.374	–
Ease of injection (Likert scale). Median [IQR]	3 [1]	3[1]	5 [0]	2 [1]	2 [1]	2 [2]	4[0]	4.5 [0.5]	**0.009**	–
Residual aqueous phase (%). Median [IQR]	33.9 [16.1]	34.9 [21]	37.5 [22.7]	30.1 [21.2]	28.7 [27]	29.2 [16.8]	31.4 [8.77]	17.3 [25.9]	0.837	–
Volumetric yield (%). Median [IQR]	100 [9.5]	35 [2]	64 [10]	80 [14]	64 [20]	56.5 [25]	70 [4.5]	80 [8]	**<0.0001**	Tulip Nanofat Kit> Adinizer (p=0.0002) Lipomine > Adinizer (p=0.007) Tulip Nanofat Kit> Puregraft Boost V1 (p = 0.01) Emulsfat > Adinizer (p=0.02)

Fig. 2. Technical performance evaluation of eight devices for nanofat production. (**A**) Schematic radar plot illustrating the parameters included in the scoring system: preparation time, ease of emulsification, ease of injection, volumetric yield, and residual aqueous phase. Each parameter was scored on a 0–5 scale on a radar plot. (**B**) Radar plots showing the individual performance profiles of the eight commercially available nanofat preparation devices and the total score in blue under the radar plot. For each device, higher values indicate better performance for the given parameter. (**C**) Comparative analysis of the five technical parameters among nanofat preparation devices. Data are presented as median [interquartile range]. Kruskal–Wallis and post-hoc tests were applied to assess significant differences among devices.

lowest residual aqueous fraction proportion (17.3 [25.9]), indicating more effective fat concentration. These data highlight significant differences in workflow optimization and nanofat recovery across devices. Emulsfat and Puregraft Boost V2 obtained the highest technical scores with a total of 4.5 and 4.25 respectively. Notably, occasional kit obstruction prevented the production of nanofat under optimal conditions in the study, which occured twice with Microlyzer, twice with Emulsfat, twice with LipoCube Nano and once with Tulip Nanofat Kit.

A detailed comparative analysis of the five technical parameters among nanofat preparation devices are presented in Fig. 2C. Kruskal–Wallis and post-hoc tests revealed significant differences in preparation time between Hy-Tissue Nanofat and Puregraft Boost V2 (Kruskal–Wallis : $p = 0.012$, Dunn's test : $p = 0.026$) and major differences in volumetric yield ($p < 0.0001$), indicating statistically lower outcomes with Adinizer over Tulip Nanofat kit, Microlyzer and Emulsfat and Puregarft Boost v1 over Tulip Nanofat kit. The ease of injection was significantly different between devices (Kruskal–Wallis, $p = 0.009$). However, post hoc pairwise comparisons did not reveal significant differences between individual devices, suggesting that the effect was global rather than driven by a specific comparison.

Evaluation and comparative ranking of SVF cells isolated from nanofat using different commercial systems

The biological scores and radar plots for each device (Fig. 3A,B) are quite comparable across devices with scores ranging from 2 for Hy-Tissue Nanofat to 3.75 for Adinizer over 5. The cell viability did not reveal significant difference across devices, showing the highest viability (95.9% (10.2]) for Adinizer followed by Tulip Nanofat Kit (91.4% [11.1]), whereas the maximal nucleated viable cell yields per cc of nanofat was more variable with LipoCube Nano (721,067 VNC/cc [283,067]) and Puregraft Boost V2 (657,250 VNC/cc [193,150]) reaching the highest yield whereas Hy-Tissue Nanofat was the only device with a median yield below 100,000 VNC per cc of nanofat. The proportion of ASC ranged from 10.6% to 20% across devices with Puregraft Boost V2 and Emulsfat as top-performing devices. In terms of leukocytes content, Hy-Tissue Nanofat presented the highest proportion (45.4% [26.3]), while Microlyzer remained lower (27.5% [16.3]). The in vitro functional CFU-F assay

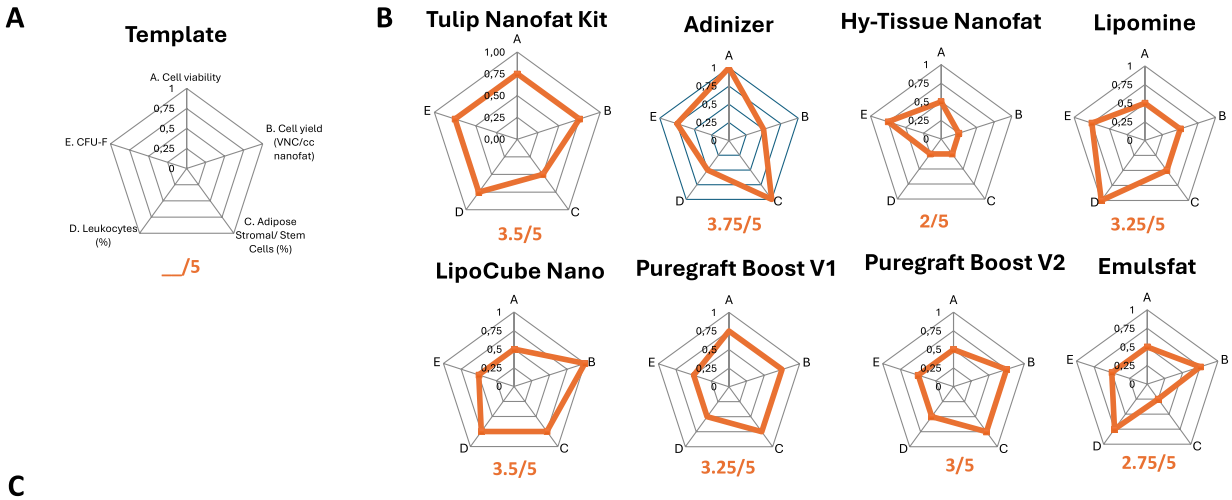

C

Parameter	Tulip Nanofat (n=5)	Adinizer (n=5)	Hy-Tissue Nanofat (n=5)	Lipomine (n=5)	LipoCube Nano (n=5)	Puregraft Boost V1 (n=4)	Puregraft Boost V2 (n=4)	Emulsfat (n=5)	*p*-value (Kruskal-Wallis)	Significant post-hoc *p*-value
Biological parameters										
Cell viability (%). Median [IQR]	91.4 [11.1]	95.9[10.2]	85.6 [18.4]	86.4 [12]	87.1 [7.1]	88 [9.3]	86 [7.6]	85.8 [11.7]	0.451	_
Cell yield (VNC/cc nanofat). Median [IQR]	644.700 [293.359]	380 267 [216 342]	55 307 [55 465]	394 450 [190 208]	721 067 [283 067]	539 250 [326 375]	657 250 [193 150]	576 300 [526 941]	**0.0031**	Lipocube> Hy-Tissue Nanofat (p = 0.006) Puregraft Boost V2 > Hy-Tissue Nanofat (p = 0.025)
Adipose Stromal/ Stem Cells (%). Median [IQR]	13.8 [4.5]	20 [6]	10.6 [6.5]	11.9 [8.6]	14.6 [2.8]	15.6 [3.8]	14.8 [5.7]	11.2 [9.4]	**0.0462**	Adinizer> Hy-Tissue Nanofat (p=0.021)
Leukocytes (%). Median [IQR]	28.6 [12.3]	45.4 [26.3]	51.6 [17.7]	27.5 [16.3]	31.7 [22.5]	37.7 [20.6]	40.8 [17.7]	35 [7.9]	**0.0496**	Hy-Tissue Nanofat >Tulip Nanofat Kit (p=0.031)
CFU-F (%). Median [IQR]	2.7 [2.15]	3.5 [3.1]	2.35 [5.3]	2.5 [3.9]	2.5 [3.2]	3.3 [4.8]	3.3 [1.6]	31 [4.7]	0.973	_

Fig. 3. Biological performance evaluation of eight devices for nanofat production. (**A**) Schematic radar plot illustrating the parameters included in the scoring system: cell viability, cell yield (viable nucleated cells/cc nanofat), proportion of adipose stromal/stem cells, proportion of leukocytes and CFU-F. Each parameter was scored on a 0–5 scale on a radar plot. (**B**) Radar plots showing the individual performance profiles of the eight commercially available nanofat preparation devices and the total score in orange under the radar plot. For each device, higher values indicate better performance for the given parameter. (**C**) Comparative analysis of the five biological parameters among nanofat preparation devices. Data are presented as median [interquartile range]. Kruskal–Wallis and post-hoc tests were applied to assess significant differences among devices.

revealed conform (> 1% for all experiments) and comparable results for all devices. A detailed comparative analysis of the five biological parameters among nanofat preparation devices are presented as median [IQR] in Fig. 3C. Kruskal–Wallis and post-hoc (Dunns) tests showed significant differences in NVC yields per cc of nanofat (Kruskal–Wallis: $p = 0.031$), and percentages of ASC and leukocytes (Kruskal–Wallis: $p = 0.0462$ and 0.0496 respectively) across devices.

Extracellular vesicle quantification and subtype distribution across nanofat preparation methods

The preparation of CM and the gating strategy used to identify large EVs (ranging from 0.16 to 0.5 µm) and to discriminate specific EVs subtypes is detailed in Fig. 4A,B.

As shown in supplementary Table S1 and summarized in Fig. 4C, total EVs concentrations ranged from 41,533 [46,740] (Tulip Nanofat Kit) to 79,417 [57,236] EVs/µL (Hy-Tissue Nanofat). These results suggest that the total EVs yield is not significantly influenced by the mechanical preparation method (Kruskal–Wallis, $p > 0.999$). Notably, the large standard deviations observed across all methods point to marked inter-donor variability, indicating that donor-specific factors seem to have a greater impact on EVs production than the processing protocol itself. Despite this variability, the analysis of EVs subpopulations repartition revealed consistent phenotypic profiles across methods. As shown in Fig. 4D and supplementary Table S2, the percentages of adipocyte-derived EVs (AEVs), platelet-derived EVs (PEVs), and adipose mesenchymal stromal/stem cell-derived EVs (MSC-EVs) were consistently the most abundant subtypes. In contrast, leukocyte-derived EVs (LEVs) and erythrocyte-derived EVs (ErEVs) were less represented, while endothelial-derived EVs (EEVs) displayed intermediate levels, with no significant differences between preparation methods. However, the percentage of AEVs was significantly higher in Emulsfat (8.98 [6.80]) compared to both Adinizer (4.97 [4.52]) and Hy-Tissue Nanofat (4.48 [5.34]).

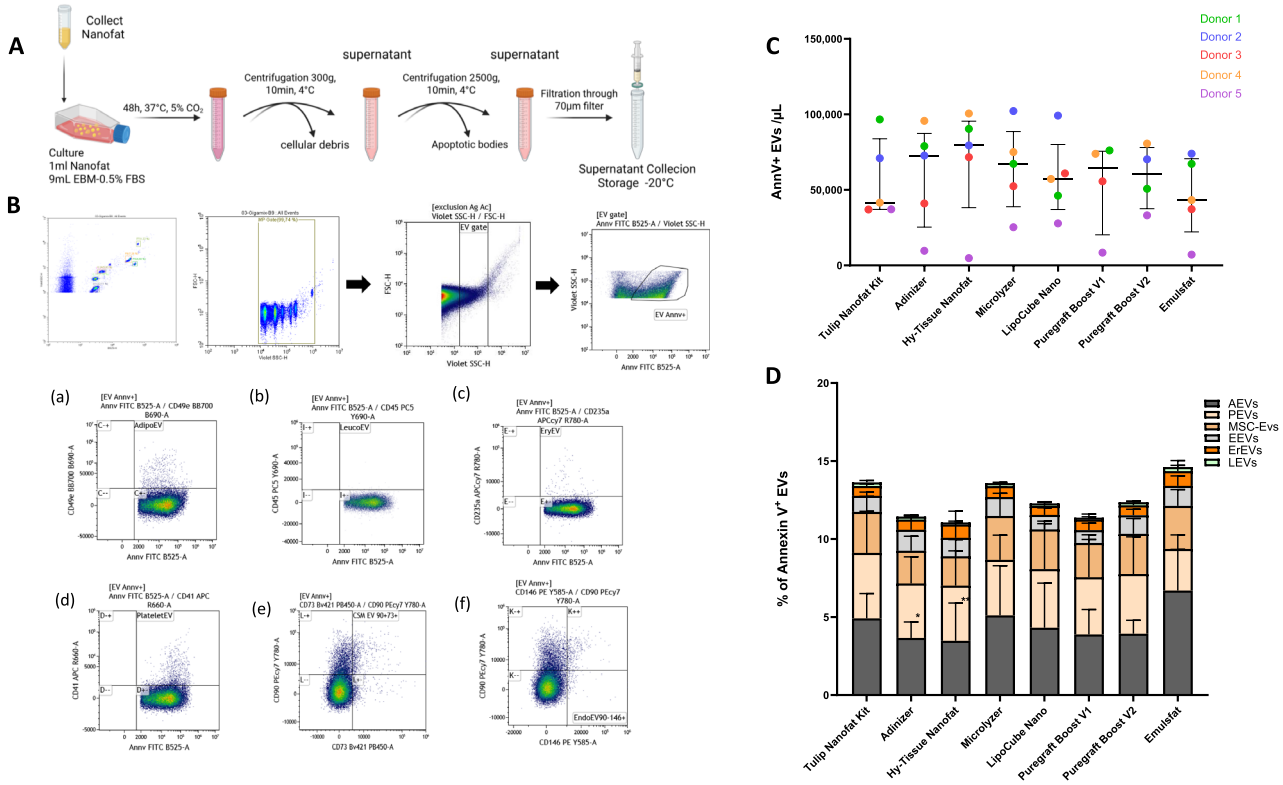

Fig. 4. Nanofat conditioned media collection and EV characterization. (**A**) Preparation of nanofat conditioned media (CM). Nanofat (1 mL) were cultured during 48 h in EBM 0,5% FBS (9 mL). CM was collected and purified by serial centrifugation and then filtered (70 µm). (**B**) Flow cytometry gating strategy used to identify large EVs (0.16–0.5 µm) and to discriminate EV subtypes on the basis of Annexin V and lineage-specific markers**.** EVs were first gated based on Annexin V expression to identify phosphatidylserine-positive EVs. Subsequent gating was performed to distinguish specific subpopulations allowing a detailed phenotyping of EV subtypes based on their surface marker expression. (a) $CD49e^+$: adipocyte-derived EVs, (b) $CD45^+$: leukocyte-derived EVs, (c) $CD235a^+$: erythrocyte-derived EVs (d) $CD41^+$: platelet-derived EVs, (e) $CD90^+$ $CD73^+$: adipose mesenchymal stromal/stem cell (MSC)-derived EVs and (f) $CD90^-$ $CD146^+$: endothelial-derived EVs. (**C**) Scatter plot showing EV concentration (EV AnnV+/µl) obtained from nanofat-derived secretome (n = 8 devices for nanofat production) across five healthy donors. Each color corresponds to a specific donor (n = 5). (**D**) Stacked bar plots showing the proportional distribution of each EV subtype within the Annexin V^+ EV population (expressed as percentage of gated Annexin V^+ EVs). This representation highlights the relative enrichment of AEVs in Emulsfat compared to Adinizer and Hy-Tissue Nanofat. Error bars represent standard deviation, and statistically significant differences in AEV proportions are marked ($^*p \leq 0.05$, $^{**}p \leq 0.01$). Figure created with BioRender.com.

Mature adipocytes and an intact vascular network persist within nanofat

Adipocyte size and distribution, as well as the endothelial network and laminin expression were assessed to evaluate the viability and structural integrity of the samples. Owing to the very low cellular yield and the presence of numerous lipid droplets, these analyses could not be performed on the nanofat produced using the Hy-Tissue Nanofat system.

First, qualitative and quantitative confocal microscopy analyses revealed that, compared to millifat, microfat resulted in lower levels of all the measured parameters (Fig. 5), suggesting that the protocol for lipoaspirates (i.e. the cannula used for adipose tissue collection) may influence adipocyte size, as well as laminin content and vascular network composition. All the medical devices used for processing adipose tissue were effective in preserving mature adipocytes, with a minimal mean size of 45 µm and a maximum diameter above 120 µm (Fig. 5A, B). Tulip Nanofat Kit and Puregraft Boost V2 resulted in a reduction in the mean size of adipocytes (45 µm and 47 µm, respectively) when compared to millifat (mean diameter 69 µm). Other devices had a marginal impact on the overall adipocyte distribution. The Microlyzer device showed a decrease number of adipocytes when compared to the other devices and Emulsfat reduced the mean size of adipocytes when comparing microfat with a distribution size of 49 µm and 63 µm, respectively.

With respect to the endothelial network, all devices preserved the network but with weak variations in vessel size and overall network density. Quantitative analysis of the total positive volume for CD31 staining revealed that the Adinizer and Microlyzer devices resulted in a slight reduction in the total CD31 positive volume compared with the millifat, yet they maintained the integrity of larger vessels (Fig. 5C).

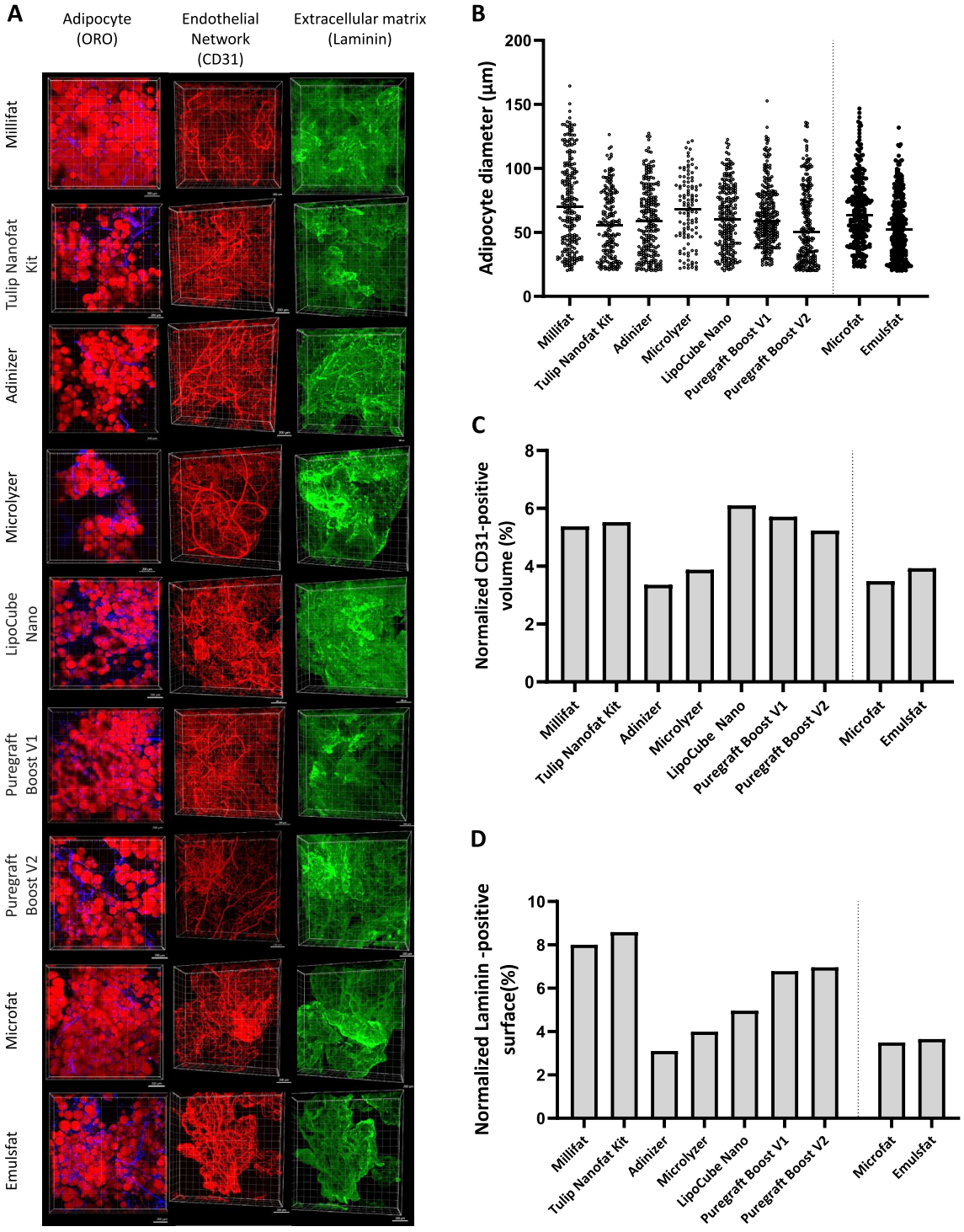

Fig. 5. Structural analysis of human microfat, millifat and nanofat. (**A**) Representative 3D confocal reconstructions showing the spatial organization of adipocytes (ORO, red), endothelial networks (CD31, red), and extracellular matrix (Laminin, green) in bioengineered adipose tissues after treatment with different device. Nuclei are stained with Hoechst (blue). Images highlight differences in adipocyte morphology, vascularization, and ECM deposition across conditions. Scale bars = 200 µm. (**B**) Quantitative analysis of adipocyte diameter distribution across conditions (n = 1). (**C**) Quantitative analysis of endothelial network density (CD31 positive signal, n = 1). (**D**) Quantification of laminin-positive extracellular matrix content (n = 1).

Regarding the extracellular matrix (ECM) integrity, as assessed by laminin expression, we have seen that all devices displayed preserved ECM structure and staining density. However, a reduction in the ECM volume was observed with all devices except the Tulip Nanofat Kit (Fig. 5D). Our immunofluorescent assessment of ECM preservation was limited to laminin, a basement membrane marker. Notably, although limited to a single donor, $CD31^+$ volume and $laminin^+$ surface area appeared similar between nanofat prepared with the Emulsfat system and the initial microfat sample.

Discussion

This study provides the first comprehensive comparative analysis of nanofat obtained from eight commercially available preparation devices, integrating both their technical performance and biological characterization. The donor population was relatively homogeneous, comprising healthy adult female patients undergoing elective surgery, with AT (including macro- and microfat) harvesting procedures performed by the same surgeon. Whereas most previous studies focused on only two systems for nanofat production or a limited number of biological endpoints, this study integrates a broader evaluation of eight commercial devices. Notably, the results revealed notable differences between their technical handling and biological quality.

From a technical standpoint, Emulsfat and Puregraft Boost V2 stood out with the highest technical scores (4.5 and 4.25, respectively), indicating that they are efficient, user-friendly devices requiring minimal force and intuitive handling. In contrast, LipoCube Nano and Puregraft Boost V1 had lower technical scores (2.75 and 3.0), reflecting more complex or resistant handling. This emphasizes that design adaptations made by Bimini Healthcare significatively improved the technical performance from the first version V1 to the second version of the Puregraft Boost system[18].

The absence of standardized terminology combined with the wide variability in preparation protocols — including differences in the number of emulsification/micronization passes and the type of filtration systems used continues to hinder and interpretation of results and comparison of the different procedures. To overcome this limitation, our team recently reported responses from a panel of experts, who proposed that nanofat refers to lipoaspirate that benefits from a washing step, followed by emulsification (20–30 passes) with a connector size between 1.2 and 1.6 mm, and a terminal step of filtration with a pore size of approximately 300–500 µm[21]. According to this definition, only three of the devices assessed in our study—Tulip Nanofat Kit, LipoCube Nano, and Emulsfat—met these criteria. The experts also agreed that nanofat can be produced through micronization using blades[18], as in four of the evaluated commercial devices of the study, but none of these include a final filtration step.

From a biological perspective, the ranking of the eight systems differed. Adinizer achieved the highest biological evaluation (3.75), suggesting superior preservation or regenerative cell recovery, whereas Emulsfat—technically optimal—received only moderate biological ratings (2.75). Hy-Tissue Nanofat scored the lowest in terms of biological quality[2], despite being technically comparable to several other kits. These findings also highlight the possible dissociation between technical ease and biological performance; while handling performance and volumetric yield are critical in clinical settings, it does not necessarily correlate with optimal biological preservation. Therefore, the choice of device may need to be tailored according to the priority given to handling versus clinical objective. Moreover, most published in vitro studies on nanofat have relied on non-commercial preparation methods, further complicating comparisons across studies. Nevertheless, our findings are consistent with those of Cohen et al., who compared the LipoCube Nano and Tulip Nanofat Kit devices and observed superior biological outcomes with LipoCube Nano, notably higher cell yields and greater proportions of ASC, despite comparable cell viability between the two systems[11].

Qiu et al. compared biological features of different nanofat samples prepared with 5 different convertor sizes (ranging from 3.76 to 0.8 mm) and demonstrated that processing parameters can significantly affect the regenerative cell content and secretory profile of nanofat[24]. Using fat converters with smaller diameters led to a significant decrease in the total number of SVF cells, with no significant impact on their viability, suggesting that the mechanical stress induced by narrower converters reduce regenerative cell yields during the emulsification process. Interestingly, the pro angiogenic activity was reduced with the SVF obtained from the smaller aperture converter (1.20 mm, 1.00 mm, 0.80 mm) with cells from large aperture size retained their ability to achieve the formation of capillary-like structures in the Matrigel assays. In line with this, histological analyses in this study showed a slight reduction in vascular density with the Adinizer and Microlyzer devices, whose final connector diameters were 0.4 and 0.6 mm respectively. Owing to its small terminal filtration pore size (120-µm), Hy-Tissue Nanofat produces a nanofat with an elevated oil content but poor cellular recovery with a median of approximately 55,000 cells/cc, confirming the results of another study evaluating this device[11]. In line with this, the oil droplet content is known to increase with smaller connectors size[24] or pore filtration, as with Hy-Tissue Nanofat device. Moreover, Hy-Tissue Nanofat device led to high cell viability but it also contained a large proportion of cellular debris compared with the other systems (DRAQ5-negative events, *data not shown*) which could be linked to the final filtration step, as this kit features the smallest terminal filter diameter among the devices studied.

Grünherz et al. reported that, from 109 biological pathways, anti-inflammatory, anti-fibrotic and anti-melanogenic lipid mediators were particularly enriched in nanofat prepared using the Tulip Nanofat Kit when compared with unprocessed AT[25]. Furthermore, proteomics analysis, revealed that upregulated genes in nanofat are involved in innate immune responses, coagulation, and wound healing, whereas downregulated genes were associated with cellular migration and extracellular matrix production without affecting the concentration of tissue regeneration biomarkers[26]. These findings highlight the strong influence of processing methods on the biological functionality of nanofat.

In our recent systematic review on nanofat[18], we highlighted its growing use in regenerative medicine, including head and neck reconstruction, facial rejuvenation, wound healing, and scar management. Future

indications should also be explored, particularly in the orthopaedic domain and in soft-tissue reconstruction, such as volume restoration, post-radiation injury, or fistula repair. Our integrated scoring system aims to synthesise multiple technical or biological parameters and may help clinicians identify which device best aligns with the requirements of a given clinical application. For instance, devices that displayed high ASC proportion and cell viability in our study, might be more suitable for cell-rich regenerative applications, whereas systems with easy injectability, short preparation time, and high-volume yield could be advantageous for procedures targeting superficial tissue regeneration or scar treatment.

We also demonstrated that vascular networks and extracellular matrix were maintained by immunofluorescence imaging, even on one sample set. This is an important observation, in contrast with the existing literature where mechanical processing is often associated with complete adipocyte destruction and matrix disruption. This study provided refined microscopic evidence of the persistence of adipocyte structures within nanofat, with small lobules variably preserved across devices. This raises the question of whether "nanofat" is an appropriate term, given that the final products still contain adipocytes, microvascular fragments, and extracellular matrix components, none of which fall within the nanoscale. This observation echoes recent expert-consensus reflections, which similarly failed to reach agreement on the suitability of the term[18]. Nevertheless, because "nanofat" has been widely adopted in the international literature since its original description by Tonnard in 2013[7], we retained this terminology for consistency with current usage.

Besides, it remains important not to overlook the potential paracrine effects of nanofat, particularly those mediated by EVs that may be generated during the processing steps. Indeed, EVs may act as key mediators of the paracrine effects of nanofat, delivering growth factors, cytokines, and microRNAs that contribute to angiogenesis, immune modulation, and tissue regeneration[27,28]. Here, we report the first detailed comparative analysis of EVs in nanofat secretomes, using a flow cytometry strategy adapted from SVF gating protocols[29]. EVs concentrations seemed to be consistent across devices (no statistical difference between devices) and seemed to be mainly influenced by donor factors (given the consistency between the levels of EVs in each patient across the devices). However, although the secretome of Emulsfat was relatively enriched in adipocyte-derived EVs. These findings suggest that certain methods may preferentially enrich specific EVs subtypes, possibly due to differences in the mechanical forces or due to the starting AT lipoaspirates (microfat for Emulsfat and millifat for other systems). We did not use EV-depleted FBS in the culture medium; however, we minimized FBS content (0.5%) and used human-specific markers to largely distinguish human-derived EVs from any bovine vesicles. Additionally, our study was restricted to EV characterization; we did not assess other soluble factors (e.g., cytokines, growth factors) in the nanofat secretome. Ultimately, donor variability appears to be a more influential factor than emulsification method in determining the distribution of EV subtypes in this model.

Study limitations include the relatively small number of donors (n = 5) and the limited number of samples per device for histological evaluations (n = 1), allowing only descriptive analysis for microarchitecture analysis whereas we did not assess physicochemical properties of the obtained products. Moreover, only laminin staining was used for ECM characterization, other components (e.g., collagens, fibronectin) may also be relevant to tissue integrity post-processing. Future analyses using a broader panel of ECM markers would be valuable to confirm how comprehensively the matrix is preserved in nanofat preparations.

In addition, comparisons are also complicated by the use of microfat as a starting material for Emulsfat as recommended by the manufacturer, whereas all other devices processing millifat, part of the variance in outcomes (e.g. adipocyte -derived EV enrichment) may therefore reflect input material rather than device performance. Besides, we focused here on the EV characterization within the secretome and we therefore did not assess soluble factors. This focus was motivated by previous studies reporting no major differences in soluble factor profiles across nanofat manufacturing methods, whereas the EV compartment has, to our knowledge, not yet been systematically investigated. Finally, no functional assays were performed, so it remains uncertain whether the observed cellular and secretome differences translate into clinically relevant regenerative outcomes. Further investigations and additional functional assays are needed to validate the reproducibility of these results across larger cohorts.

Conclusions

Overall, the combined technical and biological profiling presented here provides a valuable framework for guiding the selection of nanofat preparation devices according to specific clinical objectives, whether emphasizing the cellular content or viability, or the technical performance such as volumetric yield. These insights also pave the way for refining nanofat processing techniques on the basis of biological criteria to maximize therapeutic outcomes.

Data availability

All data generated during this study are included in this published article. The data that support the findings of this study are available on request from the corresponding author, upon reasonable request.

Received: 28 October 2025; Accepted: 16 February 2026
Published online: 20 February 2026

References

1. Coleman, S. R. Structural fat grafting: More than a permanent filler. *Plast. Reconstr. Surg.* **118**(Suppl), 108S-120S (2006).
2. Meruane, M. A., Rojas, M. & Marcelain, K. The use of adipose tissue-derived stem cells within a dermal substitute improves skin regeneration by increasing neoangiogenesis and collagen synthesis. *Plast. Reconstr. Surg.* **130**(1), 53–63 (2012).
3. Zuk, P. A. et al. Multilineage cells from human adipose tissue: Implications for cell-based therapies. *Tissue Eng.* **7**(2), 211–228 (2001).

4. Nguyen, P. S. A., Desouches, C., Gay, A. M., Hautier, A. & Magalon, G. Development of micro-injection as an innovative autologous fat graft technique: The use of adipose tissue as dermal filler. *J. Plast. Reconstr. Aesthetic. Surg. JPRAS.* **65**(12), 1692–1699 (2012).
5. Ding, P. et al. Research progress on preparation, mechanism, and clinical application of nanofat. *J. Burn Care Res. Off Publ. Am. Burn. Assoc.* **43**(5), 1140–1144 (2022).
6. La Padula, S. et al. Nanofat in plastic reconstructive, regenerative, and aesthetic surgery: A review of advancements in face-focused applications. *J. Clin. Med.* **12**(13), 4351 (2023).
7. Tonnard, P. et al. Nanofat grafting: Basic research and clinical applications. *Plast. Reconstr. Surg.* **132**(4), 1017–1026 (2013).
8. Quintero Sierra, L. A. et al. Highly pluripotent adipose-derived stem cell-enriched nanofat: A novel translational system in stem cell therapy. *Cell Transplant.* **32**, 9636897231175968 (2023).
9. Grünherz, L., Sanchez-Macedo, N., Frueh, F. S., McLuckie, M. & Lindenblatt, N. Nanofat applications: From clinical esthetics to regenerative research. *Curr. Opin. Biomed. Eng.* **10**, 174–180 (2019).
10. Lo Furno, D. et al. Nanofat 2.0: Experimental evidence for a fat grafting rich in mesenchymal stem cells. *Physiol. Res.* **66**(4), 663–671 (2017).
11. Cohen, S. R. et al. Cellular optimization of nanofat: Comparison of two nanofat processing devices in terms of cell count and viability. *Aesth. Surg. J. Open Forum.* **1**(4), 28 (2019).
12. Wei, H. et al. Nanofat-derived stem cells with platelet-rich fibrin improve facial contour remodeling and skin rejuvenation after autologous structural fat transplantation. *Oncotarget* **8**(40), 68542–68556 (2017).
13. Colazzo, F. et al. Shear stress and VEGF enhance endothelial differentiation of human adipose-derived stem cells. *Growth Factors* **32**(5), 139–149 (2014).
14. Banyard, D. A. et al. Phenotypic analysis of stromal vascular fraction after mechanical shear reveals stress-induced progenitor populations. *Plast. Reconstr. Surg.* **138**(2), 237e-e247 (2016).
15. Sultan, S. M. et al. Human fat grafting alleviates radiation skin damage in a murine model. *Plast. Reconstr. Surg.* **128**(2), 363–72 (2011).
16. Klinger, M., Caviggioli, F., Vinci, V., Salval, A. & Villani, F. Treatment of chronic posttraumatic ulcers using autologous fat graft. *Plast. Reconstr. Surg.* **126**(3), 154e-e155 (2010).
17. Rageh, M. A., El-Khalawany, M. & Ibrahim, S. M. A. Autologous nanofat injection in treatment of scars: A clinico-histopathological study. *J. Cosmet. Dermatol.* **20**(10), 3198–3204 (2021).
18. Arcani, R. et al. Nanofat use in regenerative medicine: A systematic literature review and consensus recommendations from expert opinions. *Facial Plast. Surg. Aesth. Med.* **1**, 1 (2025).
19. Lombardo, J. A., Banyard, D. A., Widgerow, A. D. & Haun, J. B. Fluidic device system for mechanical processing and filtering of human lipoaspirate enhances recovery of mesenchymal stem cells. *Plast. Reconstr. Surg.* **151**(1), 72e–84e (2023).
20. Girard, P. et al. Modified nanofat grafting: Stromal vascular fraction simple and efficient mechanical isolation technique and perspectives in clinical recellularization applications. *Front. Bioeng. Biotechnol.* **10**, 895735 (2022).
21. Chen, X. et al. Mechanical emulsification of lipoaspirate by different Luer-Lok connector changes the viability of adipose derived stem cells in Nanofat. *J. Plast. Surg. Hand Surg.* **54**(6), 344–351 (2020).
22. Bourin, P. et al. Stromal cells from the adipose tissue-derived stromal vascular fraction and culture expanded adipose tissue-derived stromal/stem cells: A joint statement of the International Federation for Adipose Therapeutics and Science (IFATS) and the International Society for Cellular Therapy (ISCT). *Cytotherapy* **15**(6), 641–648 (2013).
23. Bonifay, A. et al. A new strategy to count and sort neutrophil-derived extracellular vesicles: Validation in infectious disorders. *J. Extracell. Vesicles* **11**(4), 1. https://doi.org/10.1002/jev2.12204 (2022).
24. Qiu, H., Jiang, Y., Chen, C., Wu, K. & Wang, H. The effect of different diameters of fat converters on adipose tissue and its cellular components: selection for preparation of nanofat. *Aesth. Surg. J.* **41**(11), 1734–1744 (2021).
25. Grünherz, L., Kollarik, S., Sanchez-Macedo, N., McLuckie, M. & Lindenblatt, N. Lipidomic analysis of microfat and nanofat reveals different lipid mediator compositions. *Plast. Reconstr. Surg.* **154**(5), 895e–905e (2024).
26. Sanchez-Macedo, N., McLuckie, M., Grünherz, L. & Lindenblatt, N. Protein profiling of mechanically processed lipoaspirates: Discovering wound healing and antifibrotic biomarkers in nanofat. *Plast. Reconstr. Surg.* **150**(2), 341e-e354 (2022).
27. Chen, A. et al. Small extracellular vesicles from human adipose-derived mesenchymal stromal cells: A potential promoter of fat graft survival. *Stem Cell Res. Ther.* **12**(1), 263 (2021).
28. Wang, Y., Li, Q., Zhou, S., & Tan, P. Contents of exosomes derived from adipose tissue and their regulation on inflammation, tumors, and diabetes. *Front. Endocrinol.* **15**, 1374715 (2024).
29. François, P. et al. Inter-center comparison of good manufacturing practices-compliant stromal vascular fraction and proposal for release acceptance criteria: a review of 364 productions. *Stem Cell Res Ther.* **12**(1), 373 (2021).

Acknowledgements

The authors declare that they have not used AI-generated work in this manuscript

Author contributions

RA, MA, SS, VD, SR, AZ, LA, CB, SM and MV performed experiments and collected data. RA, SS, VD, SR, EJ, LA, RL, MV and JM analysed and interpreted the results. GM, AD, MV, and JM conceived the study, supervised the project, and contributed to data interpretation. GM, RL, FDG, FS, and AD provided critical input on study design, data interpretation, and manuscript revision. RA, MA, SS, SR, LA, VD, MV and JM drafted the manuscript. All the authors have read and approved the final version of the manuscript.

Funding

This study was funded by the Société Nationale Française de Médecine Interne (SNFMI) and the Association des Hospitalo-Universitaires de Marseille (ASHUM).

Declarations

Competing interests

GM, FS and JM are cofounders of the Remedex Network. JM received honoraria for educational support from Fidia Pharmaceuticals, Horiba, Arthrex, Horus Pharma and Macopharma. These manufacturers had no role in the development of this study or its decision for publication. The authors declare that they have no competing interests.

Ethics approval and consent to participate

All donors who participated in the study received an information and nonopposition notice and did not express any objection to the use of their adipose tissue.

Additional information

Supplementary Information The online version contains supplementary material available at https://doi.org/10.1038/s41598-026-40847-2.

Correspondence and requests for materials should be addressed to J.M.

Reprints and permissions information is available at www.nature.com/reprints.

Publisher's note Springer Nature remains neutral with regard to jurisdictional claims in published maps and institutional affiliations.